AIP | The Journal of Chemical Physics

The Hessian biased force field for silicon nitride ceramics: Predictions of thermodynamic and mechanical properties for α- and β-Si3N4

John A. Wendel and William A. Goddard III

Citation: The Journal of Chemical Physics **97**, 5048 (1992); doi: 10.1063/1.463859
View online: http://dx.doi.org/10.1063/1.463859
View Table of Contents: http://scitation.aip.org/content/aip/journal/jcp/97/7?ver=pdfcov
Published by the AIP Publishing

Articles you may be interested in

Mechanical properties of β-Si3N4 thin layers in basal plane under tension: A molecular dynamics study
Appl. Phys. Lett. **102**, 031907 (2013); 10.1063/1.4788692

Vibrational wave functions and spectroscopy of (H2O) n , n=2,3,4,5: Vibrational self-consistent field with correlation corrections
J. Chem. Phys. **105**, 10332 (1996); 10.1063/1.472960

Nitrogen incorporation in thin oxides by constant current N2O plasma anodization of silicon and N2 plasma nitridation of silicon oxides
Appl. Phys. Lett. **69**, 1053 (1996); 10.1063/1.116928

Formation of β-Si3N4 by nitrogen implantation into SiC
J. Appl. Phys. **78**, 7018 (1995); 10.1063/1.360470

Reaction of organic materials with YBa2Cu3Ox
AIP Conf. Proc. **165**, 451 (1988); 10.1063/1.37078

Reuse of AIP Publishing content is subject to the terms: https://publishing.aip.org/authors/rights-and-permissions. Downloaded to IP: 133.6.143.32 On: Mon, 27 Jun 2016 08:35:53

The Hessian biased force field for silicon nitride ceramics: Predictions of thermodynamic and mechanical properties for α- and β-Si_3N_4

John A. Wendel and William A. Goddard III
California Institute of Technology (139-74), Materials and Molecular Simulation Center, Pasadena, California 91125

(Received 26 May 1992; accepted 22 June 1992)

A force field (MSXX) for molecular dynamics simulations of silicon nitride is derived using the Hessian biased technique from *ab initio* calculations on $N(SiH_3)_3$ and $Si(NH_2)_4$ clusters. This is used to model the nitrogen and silicon centers of the α and β forms of crystalline Si_3N_4 for prediction of crystal structures, lattice expansion parameters, elastic constants, phonon states, and thermodynamic properties. Experimental measurements on many of these important physical constants are lacking, so that these calculations provide the first reliable data on such fundamental properties of silicon nitride. This MSXX force field is expected to be useful for molecular dynamics simulations of dislocations and grain boundaries and for studying the reconstruction and energetics of clean, reduced, and oxidized surfaces.

I. INTRODUCTION

Silicon nitride has long been recognized as a promising high temperature structural ceramic for use in diesel engines, industrial heat exchangers, and gas turbines, to name but a few potential applications.[1] The good thermal stress, oxidation, corrosion, and erosion resistance should allow silicon nitride to operate in high temperature, high stress environments without being cooled. This is a distinct advantage over the materials currently used in these applications (the alloys of chromium, cobalt, nickel, and tungsten) which require constant cooling to avoid melting. This decreased heat loss to cooling for engines insulated with silicon nitride, leads to an increased efficiency of these engines. However, efforts to implement silicon nitride in such devices, have been frustrated by its brittleness (often leading to catastrophic fracture), problems with surface adhesion, and difficulties in processing the raw material into useful forms.[1] This latter problem has given rise to a family of silicon nitride based materials which utilize different sintering additives and hot pressing conditions to produce compounds with varying densities, α:β ratios, and intergranular structures. Most of these materials have strengths and stress resistances far below the theoretical limits.

The most commonly used sintering additives, silicates and metal oxides, tend to conglomerate at intergranular boundaries.[1] Softening of these intergranular glassy phases has been indicted as the main cause of creep and subsequent thermal breakdown in commercial materials. An atomic-level understanding of the behavior of different additives at the grain boundaries would facilitate prediction of the tribological properties of new and potentially more desirable silicon nitride based materials.

As a first step towards modeling the relevant surfaces and interfaces of commercial silicon nitrides, we have studied the basic physical properties of the pure α and β-Si_3N_4 systems. Since almost no data is available for the pure systems, we view our results as benchmarks against which future forms of silicon nitride can be compared as processing technology advances.

II. FORCE FIELDS

A. Energy expression

We found that the general energy expression (1) leads to an accurate description of these systems,

$$E=E_b+E_a+E_t+E_\psi+E_{ax}+E_{1aa}+E_{\mathrm{vdW}}+E_Q. \quad (1)$$

This includes Morse bond stretch (E_b), Cosine angle bend (E_a), dihedral angle torsion (E_t), umbrella inversion (E_ψ), bond–angle and bond–bond coupling (E_{ax}), one center angle–angle coupling (E_{1aa}), van der Waals (E_{vdW}), and electrostatic (E_Q) terms. This force field is denoted[2] as MSXX to indicate the inclusion of both E_{ax} angle cross terms (first X) and E_{1aa} additional cross terms (second X). These interactions are defined by the following energy expressions:

(i) The Morse potential for bond stretching

$$E_b=D_b[e^{-\alpha_b(R-R_b)}-1]^2, \quad (2)$$

where R is the length of the bond, R_b and D_b are the position and depth of the well, and $K_b=2D_b\alpha_b^2$ is the force constant. D_b was not adjusted (standard bond energies were used).

(ii) The harmonic cosine expansion for angle bending,

$$E_a=\tfrac{1}{2}C[\cos\theta-\cos\theta_a]^2, \quad (3)$$

where θ is the angle between bonds IJ and JK, θ_a is the equilibrium angle, and $K_\theta=C\sin^2\theta_a$ is the diagonal force constant.

(iii) Torsion terms

 0021-9606/92/195048-15$006.00 © 1992 American Institute of Physics

Reuse of AIP Publishing content is subject to the terms: https://publishing.aip.org/authors/rights-and-permissions. Downloaded to IP: 130.6.143.32 On: Mon, 27 Jun 2016 08:35:53

$$E_t=\tfrac{1}{2}V_n(1+\cos n\phi), \tag{4}$$

where ϕ is the angle between bonds IJ and KL when sighted down JK, V_n is the barrier, and $n=3$ is the period. All six torsions for any choice of JK are included with V_n renormalized to $V_n/6$.

(iv) Umbrella inversion terms, for planar atoms (N),

$$E_\psi=K_\psi(1-\cos\psi), \tag{5}$$

where, given an atom I bonded to three other atoms, J, K, and L, ψ is the angle between the bond IL and the plane IJK, and K_ψ is the force constant. The three terms using various choices of L are averaged.

(v) Bond–angle and bond–bond cross terms

$$E_{ax}=D_1(\cos\theta-\cos\theta_a)(R_1-R_{b1})+D_2(\cos\theta-\cos\theta_a)\times(R_2-R_{b2})+K_{rr}(R_1-R_{b1})(R_2-R_{b2}), \tag{6}$$

where R_1 is the length of bond IJ, R_2 is the length of bond JK, $K_{r\theta}=-D\sin\theta_a$ is the bond–angle force constant, and K_{rr} is the bond–bond force constant.

(vi) One center angle–angle inversions of the form

$$E_{1aa}=G(\cos\theta_{\mathrm{IJK}}-\cos\theta_{a\mathrm{IJK}})(\cos\theta_{\mathrm{IJL}}-\cos\theta_{a\mathrm{IJL}}), \tag{7}$$

where $K_{1\theta\theta}=G\sin(\theta_{a\mathrm{IJK}})\sin(\theta_{a\mathrm{IJL}})$ is the force constant for two angle terms, IJK and IJL, sharing a common central bond IJ and a common central atom J.

(vii) The exponential-6 potential used for the van der Waals part of the nonbond interactions

$$E_{\mathrm{vdW}_{\mathrm{IJ}}}=Ae^{-BR_{\mathrm{IJ}}}-\frac{C}{R_{\mathrm{IJ}}^6}=\frac{D_v}{(\zeta-6)}\left[6e^{\zeta(1-\rho)}-\zeta\rho^{-6}\right], \tag{8}$$

where R_{IJ} is the distance between atoms I and J, R_v and D_v are the position and depth of the well, ζ is a dimensionless parameter, and $\rho=R_{\mathrm{IJ}}/R_v$. The parameters in the van der Waals energy expression were chosen from previous studies[3–5] of other systems and were not optimized for Si_3N_4.

(viii) Electrostatic terms

$$E_Q=\frac{Q_iQ_j}{\epsilon_0\epsilon R_{ij}}, \tag{9}$$

where Q_{I} (in electron units) is the charge on atom I, $\epsilon=1$ is the dielectric constant, and $\epsilon_0=1/332.0637$ gives E_Q in kcal/mol when R_{IJ} is the distance in angstroms. Charges for the clusters $N(SiH_3)_3$ and $Si(NH_2)_4$ were obtained using the charge equilibration technique of Rappe and Goddard,[2] whereas charges for the periodic Si_3N_4 system were calculated using an extension of this basic technique to infinite systems.[6]

B. Hessian biased method (Ref. 7)

The second derivative matrix or Hessian, (10), determines the vibrational frequencies (phonons) and elastic constants (Young's moduli, Poisson ratios) for a molecule or crystal

$$H_{ij}=\frac{\partial^2E}{\partial R_i\,\partial R_j}. \tag{10}$$

Here R_i are the $3N$ atomic coordinates. The Hessian is obtained directly from *ab initio* Hartree–Fock calculations. To obtain vibrational frequencies (ν_i) the mass weighted Hessian (11)

$$H_{ij}^{\mathrm{MW}}=H_{ij}(M_iM_j)^{-1/2} \tag{11}$$

is diagonalized to obtain

$$\mathbf{H}^{\mathrm{MW}}\mathbf{U}=\mathbf{U}\lambda, \tag{12}$$

where the diagonal matrix λ holds the eigenvalues of $\mathbf{H}^{\mathrm{MW}}$ and the columns of $\mathbf{U}$ hold the modes. The vibrational frequencies in cm^{-1} are then obtained from

$$\lambda_i=\kappa(\nu_i)^2, \tag{13}$$

where $\kappa=8.480\,27\times10^{-5}$ if masses are in atomic mass units ($^{12}C=12.000$), energies are in kcal/mol, and distances are in A.

The Hartree–Fock method, however, tends to overestimate vibrational frequencies by 10%–20%, since it does not account for the static and dynamic electron correlation effects which change as the nuclei are moved. Fitting a force field to match the theoretical Hessian would result in force constants which are too large. Hence, the Hessian is biased with experimental data by replacing the theoretical frequencies in λ with the experimental frequencies λ^{exp}. The experimentally biased Hessian, defined as

$$\mathbf{H}^{\mathrm{EBH}}=\mathbf{U}\lambda^{\mathrm{exp}}\tilde{\mathbf{U}}, \tag{14}$$

has the property that diagonalization leads to the theoretical vibrational modes and the experimental vibrational frequencies. We then adjust the parameters in the force field, (1), to reproduce the experimentally biased Hessian (15b) and the experimental geometry (15a) as closely as possible. This leads to a total of $M+M(M-1)/2=M(M+1)/2$ conditions (where $M=3N-6$ and N is the number of atoms) for obtaining the optimal force field

$$\frac{\partial E^{\mathrm{FF}}}{\partial R_i}=0, \tag{15a}$$

$$\frac{\partial^2E^{\mathrm{FF}}}{\partial R_i\,\partial R_j}\approx H_{ij}^{\mathrm{EBH}}. \tag{15b}$$

Reuse of AIP Publishing content is subject to the terms: https://publishing.aip.org/authors/rights-and-permissions. Downloaded to IP: 133.6.143.32 On: Mon, 27 Jun 2016 08:35:53

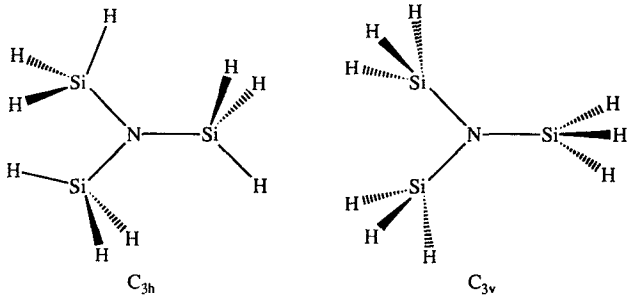

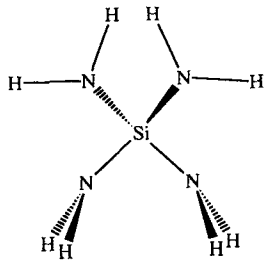

FIG. 1. The $N(SiH_3)_3$ and $Si(NH_2)_4$ structures.

TABLE I. Optimized geometric parameters for trisilylamine (Fig. 1). Hartree–Fock with the 6–31G** basis.

	C_{3h}	C_{3v}
Si–N	1.7442 Å	1.7480 Å
Si–H	1.4764 Å	1.4757 Å
Si–N–Si	120.00°	119.85°
H–Si–N	110.36°	110.37°
H–Si–H	108.57°	108.56°
Energy (Hartree)	−926.502 097	−926.500 002

C. Cluster calculations

1. $N(SiH_3)_3$

Since there has been some debate in the literature on the geometry of $N(SiH_3)_3$,[8,9] we performed *ab initio* geometry optimizations on both the C_{3v} and C_{3h} structures, which are shown schematically in Fig. 1. All calculations used the GAUSSIAN 90 program[10] with the valence double zeta plus polarization basis (6–31G**), which places a set of *p* polarization functions on H and *d* polarization functions on N and Si. We find that the C_{3h} structure is more stable than the C_{3v} structure by 1.31 kcal/mol, in agreement with the majority of experimental data. To test for planarity at the nitrogen center, the SiH_3 groups were initially bent 3° out of the plane for the C_{3h} structure (this reduces the symmetry to C_3) and 5° for the C_{3v} structure. Reoptimization led to an angle of 0.03° for the C_{3h} case and 2.3° for the C_{3v} case. The delocalization of the nitrogen lone pair into the unoccupied *d* orbitals of silicon seems to be responsible for this observed preference towards planarity. This charge transfer is further evidenced by weak electron donor properties[11] of $N(SiH_3)_3$ and the relatively short Si–N bond length.[12] The C_{3v} structure is probably prevented from becoming perfectly planar due to steric crowding of adjacent SiH_3 groups.

The $N(SiH_3)_3$ force field was calculated[13] using the Hessian biased approach with the HF Hessian for the optimized C_{3h} structure. Geometric parameters for this structure are shown in Table I. Experimental vibrational frequency data has been obtained for $N(SiH_3)_3$ down to 35 cm^{-1} and assigned by Shurvell assuming a C_{3h} structure.[14] The observed spectrum is complete except for two low lying N–(SiH_3) torsional modes. We use Shurvell's estimates of 29 and 30 cm^{-1} for these modes as our experimental frequencies. (The theoretical values are 88 and 66 cm^{-1}.) The experimental, HF, and force field frequencies are compared in Table II. We have generally attempted to exclude cross terms from the force field (1) since such terms might not be transformable from the molecules to the Si_3N_4 crystal. However, we find that inclusion of the bond–bond, bond–angle, and one-center angle–angle cross terms in the $N(SiH_3)_3$ force field is necessary for an accurate description of the experimental and HF vibrational spectra. This MSXX force field is displayed in Table III.

2. $Si(NH_2)_4$

Calculation of the force field for $Si(NH_2)_4$ presented a problem since no spectroscopic data is available for this compound (which has been observed only as a transient intermediate during chemical vapor deposition of silicon

TABLE II. Frequencies for trisilylamine (C_{3h}). Frequencies are in cm^{-1}. Values in parentheses are estimated.

Mode	Sym	Expt.[a]	HF	FF	Assignment (Ref. 14)
1	*A'*	2170	2378	2165	Si–H stretch
2	*A'*	2138	2349	2149	Si–H stretch
3	*A'*	1011	1132	1004	N–Si–H bend and H–Si–H bend
4	*A'*	919	1052	918	H–Si–H bend
5	*A'*	697	708	695	N–Si–H bend
6	*A''*	493	508	494	Si–N bend
7	*A''*	2166	2350	2150	Si–N bend
8	*A''*	945	1052	917	H–Si–H bend and N–Si–H bend
9	*A''*	748	837	776	N–Si–H bend and H–Si–H bend
10	*A''*	312	201	304	NSi_2 wag (NSi_3 deformation)
11	*A''*	(29)	88	23	N–(SiH_3) torsion
12	*E'*	2163	2362	2165	Si–H stretch
13	*E'*	2146	2354	2150	Si–H stretch
14	*E'*	997	1024	1012	Si–N stretch and N–Si–H bend
15	*E'*	946	1090	942	N–Si–H bend and H–Si–H bend
16	*E'*	898	1045	917	H–Si–H bend
17	*E'*	661	734	664	N–Si–H bend and Si–N stretch
18	*E'*	195	201	195	Si–N–Si bend and Si–N stretch
19	*E''*	2152	2344	2149	Si–H stretch
20	*E''*	921	1063	917	H–Si–H bend
21	*E''*	697	759	674	N–Si–H bend
22	*E''*	(30)	66	13	N–(SiH_3) torsion

[a]Reference 14.

Reuse of AIP Publishing content is subject to the terms: https://publishing.aip.org/authors/rights-and-permissions. Downloaded to IP: 133.6.143.32 On: Mon, 27 Jun 2016 08:35:53

TABLE III. The MSXX force field for trisilylamine (C_{3h}). Units: bonds in Å, angles in degrees; K_b and $K_{r_1r_2}$ in (kcal/mol)/Å^2; K_θ in (kcal/mol)/rad^2; $K_{r_1\theta}$ in (kcal/mol)/Å rad; and D_e in kcal/mol. Values in parentheses were not optimized.

Bond stretch [Eq. (2)]		
Si–H	R_b	1.4819
	K_b	374.1682
	D_b	(71.50)
Si–N	R_b	1.7481
	K_b	528.0125
	D_b	(105.00)
Angle bend [Eqs. (3), (6)]		
Si–N–Si	θ_a	120.1804
	K_θ	54.6706
H–Si–H	θ_a	105.5138
	K_θ	68.1990
N–Si–H	θ_a	109.6690
	K_θ	117.2139
Threefold torsion [Eq. (4)]		
H–Si–N–Si	V_t	0.5575
Inversion [Eq. (5)]		
N–Si:SiSi	ψ_e	(0.00)
	K_ψ	47.2143
Angle cross terms [Eq. (6)]		
Si–N–Si	$D_{Si\theta}$	−18.8965
	K_{SiSi}	49.0204
H–Si–H	$D_{H\theta}$	−16.3415
	K_{HH}	5.6191
N–Si–H	$D_{N\theta}$	−12.1443
	$D_{H\theta}$	−17.7591
	K_{NH}	0.0844
One center angle–angle cross terms [Eq. (7)]		
$G_{SiN:HH}$		32.0631
$G_{SiH:NH}$		17.4014
van der Waals parameters [Eq. (8)]		
H	R_v	(3.0662)
	D_v	(0.0202)
	ζ	(12.0)
N	R_v	(3.9950)
	D_v	(0.1900)
	ζ	(12.0)
Si	R_v	(4.1800)
	D_v	(0.3100)
	ζ	(12.0)
Charges [Eq. (9)]		
H_s		(−0.0386)[a]
H_a		(−0.0369)[b]
N		(−0.3770)
Si		(0.2380)

[a]In NSi_3 plane.
[b]Out of NSi_3 plane.

nitride thin films).[15] To employ the Hessian biased approach, a spectrum of estimated experimental frequencies was generated by scaling the theoretical frequencies based on mode type. These mode scale factors were obtained from calculations of the frequencies for $N(SiH_3)_3$, SiH_4, and NH_3. For $Si(NH_2)_4$, we expect four Si–N stretch, eight N–H stretch, four H–N–H bend, five N–Si–N bend, eight H–N–Si bend, and four N umbrella modes. The Si–N stretch scale factor was obtained using the primary Si–N stretching modes of $N(SiH_3)_3$, ν_6 and ν_{14}, which have experimental values of 493 and 997 cm^{-1}, and theoretical values of 508 and 1024 cm^{-1}, giving scale factors of 0.9701 and 0.9739, respectively. These scale factors are expected to be similar, since they relate to the same type of mode. Whenever more than one frequency is relevant, we used the average of the individual scale factors, in this case $(0.9701+0.9739)/2=0.9720$. For the N–Si–N bend, the bending scale factors from silane, SiH_4, were used (Table IV). The average of the scale factors for the first two SiH_3 deformation modes gives an N–Si–N scale factor of 0.9121. The remaining scale factors were obtained from ammonia (frequencies in Table V), where ν_1 and ν_3 were used for the N–H stretch, ν_4 for the H–N–H and H–N–Si bends, and ν_2 for the N umbrella. The predicted frequencies for $Si(NH_2)_4$ are shown in Table VI. The HF optimized geometric parameters are in Table VII, and the optimized[13] MSXX force field is in Table VIII.

TABLE IV. Frequencies (cm^{-1}) for silane (SiH_4).

Mode	Sym	Expt.[a]	Theory	Scale factor	Assignment
1	E	914	1018	0.8978	SiH_3 deformation
2	E	975	1053	0.9259	SiH_3 deformation
3	A_1	2187	2370	0.9228	Si–H stretch
4	T	2191	2360	0.9284	Si–H stretch

[a]Reference 16.

3. Si_3N_4 crystal

The MSXX force field for Si_3N_4 crystal,[16,17] displayed in Table IX, was obtained by combining the MSXX force fields of $N(SiH_3)_3$ and $Si(NH_2)_4$.

III. CRYSTAL STRUCTURE AND LATTICE EXPANSION PARAMETERS

The crystal structure of β-Si_3N_4 was found by Wild and Jack[18] to belong to the hexagonal, centrosymmetric $P6_3/m$ space group with two formula units, or 14 atoms,

TABLE V. Frequencies (cm^{-1}) for ammonia.

Mode	Sym	Expt.[a]	Theory	Scale factor	Assignment
1	A_1	3504	3704	0.9460	N–H stretch
2	A_1	1022	1143	0.8941	NH_3 umbrella
3	E	3577	3841	0.9313	N–H stretch
4	E	1691	1811	0.9338	H–N–H bend

[a]Reference 17.

Reuse of AIP Publishing content is subject to the terms: https://publishing.aip.org/authors/rights-and-permissions. Downloaded to IP: 133.6.143.32 On: Mon, 27 Jun 2016 08:35:53

TABLE VI. Frequencies (cm^{-1}) for tetra-aminosilane, $Si(NH_2)_4$.

Mode	HF-(C_1)[b]	HF (C_{2v})	Scaled HF	MSXX	Assignment
1	235	−104[a]	−98[a]	Not fit	Si–N–H bend
2	273	101	92	152	N–Si–N bend
3	331	213	199	156	Si–N–H bend
4	331	213	199	157	Si–N–H bend
5	328	269	245	271	N–Si–N bend
6	445	301	281	261	Si–N–H bend
7	410	321	293	301	N–Si–N bend
8	411	321	293	301	N–Si–N bend
9	356	366	334	307	N–Si–N bend
10	495	664	597	651	N umbrella
11	495	664	597	651	N umbrella
12	772	730	710	703	Si–N stretch
13	543	780	702	686	N umbrella
14	555	805	724	674	N umbrella
15	845	837	782	815	Si–N–H bend
16	881	840	817	815	Si–N stretch
17	883	841	818	807	Si–N stretch
18	944	928	867	811	Si–N–H bend
19	900	958	931	970	Si–N stretch
20	1028	1030	962	958	Si–N–H bend
21	1029	1030	962	958	Si–N–H bend
22	1734	1735	1620	1621	H–N–H bend
23	1734	1735	1620	1621	H–N–H bend
24	1727	1743	1628	1624	H–N–H bend
25	1741	1743	1628	1627	H–N–H bend
26	3794	3752	3522	3518	N–H stretch
27	3794	3752	3522	3519	N–H stretch
28	3794	3754	3524	3520	N–H stretch
29	3796	3755	3525	3521	N–H stretch
30	3890	3822	3588	3593	N–H stretch
31	3892	3824	3590	3591	N–H stretch
32	3891	3825	3591	3594	N–H stretch
33	3891	3825	3591	3594	N–H stretch

[a]These calculations assumed C_{2v} symmetry with a tetrahedral geometry at the Si, whereas the molecular distances distort slightly to C_s. Thus C_{2v} is a saddle point with one negative curvature.
[b]Geometry taken from C. F. Melius and P. Ho, J. Phys. Chem. **95**, 1410 (1991).

per unit cell. Kato[19] placed the α structure in the $P3_1c$ space group and refined the cell dimensions. The lattice parameters of the α and β forms at room temperature are shown in Table X. The α structure can be described in terms of alternating β-Si_3N_4 basal planes and mirror images of this plane, generating an α unit cell twice as long in the c direction as the β cell and with twice as many formula units. We fitted the lattice expansion data[20] for α-Si_3N_4 between 300 and 2000 K at 100 K intervals to a cubic polynomial and extrapolated to 0 K to give predicted changes in room temperature lattice parameters of $\delta_a = 1.875\times10^{-8}$ Å, $\delta_c = 1.956\times10^{-8}$ Å. Since the α and β crystal structures are similar, we predict changes of similar magnitude for the β form. This highly incompressible be-

TABLE VII. Optimized geometric parameters for tetra-aminosilane (C_{2v}). Values in parentheses not optimized.

Si–N	1.7361 Å
N–H	1.0016 Å
H–N–H	105.6452°
Si–N–H	113.0697°
N–Si–N	(109.47°)
Energy (hartree)	−511.505 480

TABLE VIII. The MSXX force field for tetra-aminosilane. Units are same as in Table III. Values in parentheses were not optimized.

Bond stretch [Eq. (2)]		
N–H	R_b	1.0022
	K_b	1017.3835
	D_b	(81.00)
Si–N	R_b	1.7451
	K_b	736.5493
	D_b	(105.00)
Angle bend [Eqs. (3), (6)]		
H–N–H	θ_a	105.5258
	K_θ	96.7024
Si–N–H	θ_a	115.8827
	K_θ	48.6631
N–Si–N	θ_a	113.7037
	K_θ	106.1720
Threefold torsion [Eq. (4)]		
N–Si–N–H	V_t	0.0586
Inversion [Eq. (5)]		
N–Si:HH	ψ_e	52.7159
	K_ψ	0.0875
N–H:HSi	ψ_e	47.9625
	K_ψ	0.9525
Angle cross terms [Eq. (6)]		
H–N–H	$D_{H\theta}$	−30.8286
	K_{HH}	−2.3267
Si–N–H	$D_{Si\theta}$	−40.5868
	$D_{H\theta}$	−29.5245
	K_{SiH}	68.0814
N–Si–N	$D_{N\theta}$	−54.7625
	K_{NN}	−13.2418
One center angle–angle cross terms [Eq. (7)]		
$G_{SiN:NN}$		−0.1558
van der Waals parameters [Eq. (8)]		
H	R_v	(3.0662)
	D_v	(0.0202)
	ζ	(12.0)
N	R_v	(3.9950)
	D_v	(0.1900)
	ζ	(12.0)
Si	R_v	(4.18000)
	D_v	(0.3100)
	ζ	(12.0)
Charges [Eq. (9)]		
H		(0.1956)
N		(−0.5939)
Si		(0.8107)

Reuse of AIP Publishing content is subject to the terms: https://publishing.aip.org/authors/rights-and-permissions. Downloaded to IP: 133.6.143.32 On: Mon, 27 Jun 2016 08:35:53

TABLE IX. Force field for Si_3N_4 crystal. Units are the same as in Table III. Values in parentheses were not optimized.

		MSXX	$MSXX_\alpha$	$MSXX_\beta$	$MSXX_{\alpha\beta}$
		Bond stretch [Eq. (2)]			
Si–N	R_b	1.7481	1.7785	1.7755	1.7770
	k_b	528.0125	528.0125	528.0125	528.0125
	D_b	(105.00)	(105.00)	(105.00)	(105.00)
		Angle bend [Eqs. (3), (6)]			
Si–N–Si	θ_a	120.1804	120.1804	120.1804	120.1804
	k_θ	54.6706	54.6706	54.6706	54.6706
N–Si–N	θ_a	113.7037	113.7037	113.7037	113.7037
	k_θ	106.1720	106.1720	106.1720	106.1720
		Threefold torsion [Eq. (4)]			
N–Si–N–Si	V_t	0.5575	0.5575	0.5575	0.5575
		Inversion [Eq. (5)]			
N–Si:SiSi	ψ_e	(0.00)	(0.00)	(0.00)	(0.00)
	K_ψ	47.2143	47.2143	47.2143	47.2143
		Angle cross terms [Eq. (6)]			
Si–N–Si	$D_{Si\theta}$	−18.8965	−18.8965	−18.8965	−18.8965
	k_{SiSi}	49.0204	49.0204	49.0204	49.0204
N–Si–N	$D_{N\theta}$	−54.7625	−54.7625	−54.7625	−54.7625
	k_{NN}	−13.2418	−13.2418	−13.2418	−13.2418
		One center angle–angle cross terms [Eq. (7)]			
$G_{SiN,NN}$		−0.1558	−0.1558	−0.1558	−0.1558
		van der Waals parameters [Eq. (8)]			
N	R_v	(3.9950)	(3.9950)	(3.9950)	(3.9950)
	D_v	(0.1900)	(0.1900)	(0.1900)	(0.1900)
	ζ	(12.0)	(12.0)	(12.0)	(12.0)
Si	R_v	(4.1800)	(4.1800)	(4.1800)	(4.1800)
	D_v	(0.3100)	(0.3100)	(0.3100)	(0.3100)
	ζ	(12.0)	(12.0)	(12.0)	(12.0)
		Charges [Eq. (9)]			
Si		(0.7707)	(0.7679)	(0.7679)	
N		(−0.5776)	(−0.5759)	(−0.5759)	

havior is consistent with the observation that both forms of silicon nitride are composed of irregular networks of SiN_4 tetrahedra which are unable to undergo cooperative reorientation. The SiN_4 tetrahedra are linked such that only distortions of the tetrahedra are possible, hindering angle and bond length deformations. Jorgensen[21] finds no change in the Si–N bond length and less than 2° change in the N–Si–N angle upon applying pressures up to 2.91 GPa to α and β crystals. This is in contrast with materials such as quartz (SiO_2) in which the SiO_4 tetrahedra easily undergo cooperative reorientations to absorb stress.[22]

Theoretical α and β crystal structures were generated by starting with the experimental structures and using the MSXX force field to optimize atomic positions and lattice parameters. This led to lattice parameters that were too small by 0.12 and 0.09 Å, respectively. To obtain better experimental crystal structures, we adjusted R_b for the Si–N bond from 1.7481 to 1.7785 (α) and 1.770 (β). This single change in the original MSXX is denoted as $MSXX_\alpha$ and $MSXX_\beta$ and these adjusted force fields (see Table IX) were implemented for all of the remaining calculations in this paper. Lattice parameters at 0 K were calculated (see Table X) using these adjusted force fields. However, it is desirable for future studies to have one force field which adequately describes both the α and β structures, although it is optimal for neither. This force field, $MSXX_{\alpha\beta}$, represents a compromise in simultaneously fitting the α and β structures. As indicated in Table X, $MSXX_{\alpha\beta}$ does a good job of fitting both structures, and we will use it for future studies of all Si_3N_4 systems.

Theoretical lattice expansion curves were obtained by performing molecular dynamics (MD) runs for 20 ps at several temperatures between 5 and 2100 K. These runs were performed on extended structures whose unit cell lengths had been doubled in the a and c directions and whose atomic coordinates and lattice parameters had been

TABLE X. Lattice parameters for Si_3N_4 crystal. Units: Å for length, and degrees for angles.

	Alpha theory (0 K, MSXX)	Theory (0 K, $MSXX_\alpha$)	Theory (0 K, $MSXX_{\alpha\beta}$)	Theory[c] (300 K, $MSXX_\beta$)	Expt.[a] (300 K)
a	7.648	7.775	7.7684	7.833	7.818±0.003
b	7.648	7.775	7.7684	7.833	7.818±0.003
c	5.567	5.650	5.6460	5.694	5.591±0.004
α	90.0	90.0	90.0	90.0	90.0
β	90.0	90.0	90.0	90.0	90.0
γ	120.0	120.0	120.0	120.0	120.0
	Beta theory (0 K, MSXX)	Theory (0 K, $MSXX_\beta$)	Theory (0 K, $MSXX_{\alpha\beta}$)	Theory[c] (300 K, $MSXX_\beta$)	Expt. (300 K)[b]
a	7.502	7.618	7.6247	7.672	7.608±0.005
b	7.502	7.618	7.6247	7.672	7.608±0.005
c	2.866	2.905	2.9070	2.928	2.911±0.001
α	90.0	90.0	90.0	90.0	90.0
β	90.0	90.0	90.0	90.0	90.0
γ	120.0	120.0	120.0	120.0	120.0

[a]Reference 16.
[b]Reference 17.
[c]Molecular dynamics.

Reuse of AIP Publishing content is subject to the terms: https://publishing.aip.org/authors/rights-and-permissions. Downloaded to IP: 133.6.143.32 On: Mon, 27 Jun 2016 08:35:53

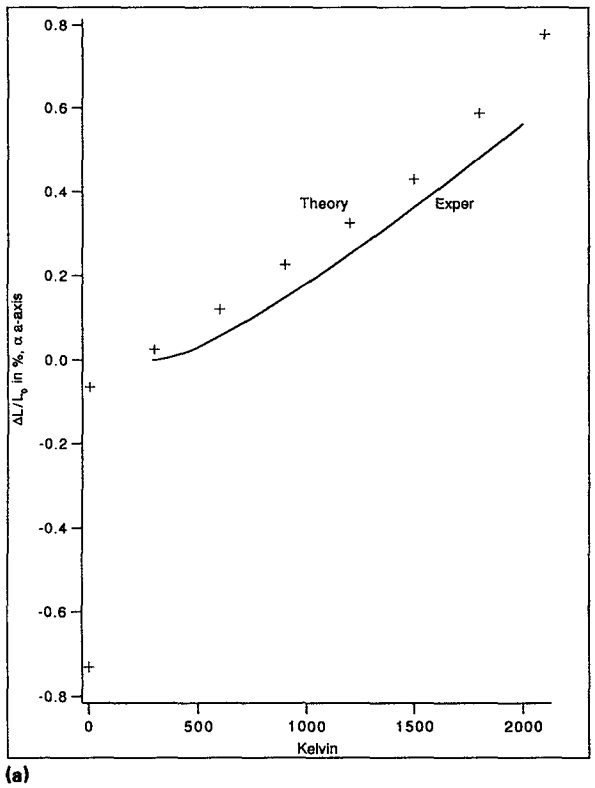

(a)

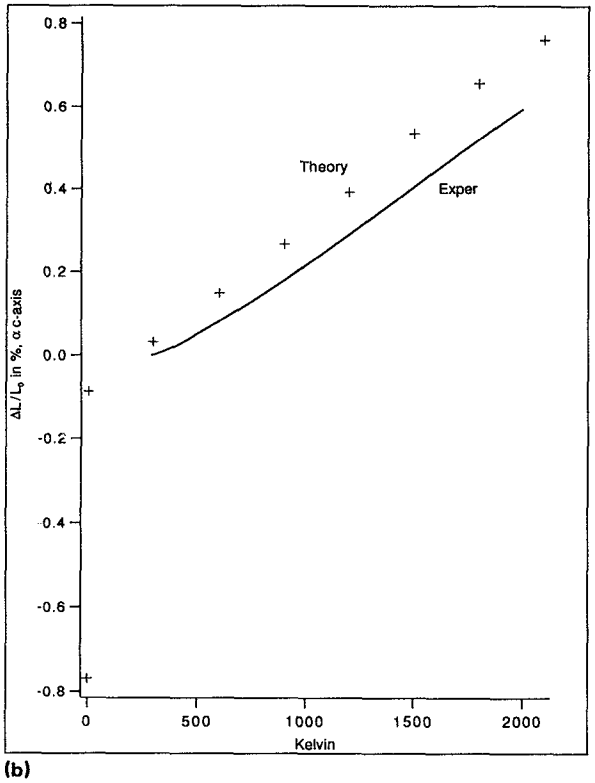

(b)

FIG. 2. Lattice expansion for α-Si_3N_4 from MD simulations; (a) A axis, (b) C axis.

minimized prior to the dynamics. Lattice constants at a given temperature were obtained by averaging over the last 15 ps of the run. The predicted thermal expansion for the a and c axes of the α structure is displayed in Fig. 2 along with an interpolation of the experimental results[19] (solid curve). The theoretical expansion behavior of our structures closely matches that of the experiment and is certainly within experimental error, $\mp 15\%$. The discontinuity in our data at 0 K is caused by the neglect of zero point motion in our classical approximation to the dynamics.

Since crystal diffraction data was collected at room temperature, the lattice constants obtained from molecular dynamics at 300 K provide the most relevant comparison with the experimental constants. These molecular dynamics averages are also shown in Table X. The theoretical results are larger than the experimental results by 0.015 to 0.103 Å with an average deviation of 0.05 Å. This indicates that the readjustment in R_b from MSXX to $MSXX_\alpha$ and $MSXX_\beta$ was slightly too large.

IV. ELASTIC CONSTANTS

Since pure single crystals of α and β silicon nitride are difficult to obtain, very little experimental data is available on the elastic moduli. The most relevant measurements were collected by Mukaseev[23] and Jorgensen.[21] Jorgensen[21] quotes unpublished[24] linear (β_a and β_c) and volume (β_v) compressibilities for α- and β-Si_3N_4. He finds $\beta_v=0.003\,90$ GPa, $\beta_a=0.001\,30$, and $\beta_c=0.001\,26$ for β-Si_3N_4 and $\beta_v=0.003\,55$, $\beta_a=0.001\,18$, and $\beta_c=0.001\,15$ for α-Si_3N_4. Mukaseev[23] determined the modulus of elasticity (Young's modulus) E along the directions $\langle 1\bar{2}12\rangle$, $\langle \bar{2}421\rangle$, and 5° to $\langle 0001\rangle$ for α-Si_3N_4 by measuring the velocity of longitudinal ultrasonic vibrations. His measurements yield $E=378$ GPa along $\langle 1\bar{2}12\rangle$, $E=488$ along $\langle \bar{2}421\rangle$, and $E=465$ along 5° to $\langle 0001\rangle$. Since these experimental measurements were carried out at room temperature, we performed calculations on a single unit cell using both the minimized 0 K structure and an expanded structure obtained from molecular dynamics at 300 K. The elastic modulus is calculated to be highly anisotropic, with the strongest direction along the c axis. Elastic constants, volume and axial compressibilities, Young's modulus, and velocities of sound are shown in Table XI.

Comparisons with experimental results have been made where possible. For a hexagonal system, there are five independent elements of the compliance matrix (s_{11}, s_{12}, s_{13}, s_{33}, and s_{44}). The elastic modulus can be related to the elements of s as follows:

$$1/E=s_{11}\sin^4\theta+s_{33}\cos^4\theta+(s_{44}+2s_{13})\sin^2\theta\cos^2\theta, \quad (16)$$

where θ is the angle between the c axis and the direction of measurement. Mukaseev[23] made three independent measurements of the elastic modulus along 5° to $\langle 0001\rangle$ ($\theta=5°$), $\langle 1\bar{2}12\rangle$ ($\theta=64.2°$), and $\langle \bar{2}421\rangle$ ($\theta=83.1°$), leading to $s_{11}=0.001\,99$ GPa, $s_{33}=0.002\,12$, $(s_{44}+2s_{13})=0.008\,44$. These results are to be compared with our theoretical values obtained at 300 K: $s_{11}=0.002\,88$ GPa, $s_{33}=0.002\,54$, $(s_{44}+2s_{13})=0.006\,59$. Also displayed in Table XI are Young's modulus along the directions of measure-

Reuse of AIP Publishing content is subject to the terms: https://publishing.aip.org/authors/rights-and-permissions. Downloaded to IP: 133.6.143.32 On: Mon, 27 Jun 2016 08:35:53

TABLE XI. Elastic constants and related quantities for Si_3N_4.

	Alpha			Beta		
	300 K	0 K	Expt.	300 K	0 K	Expt.
			Stiffness constants (GPa)			
C_{11}	426.854	436.745		439.172	447.541	
C_{12}	156.903	175.416		181.848	214.550	
C_{13}	152.039	176.016		149.909	165.140	
C_{33}	473.394	508.784		556.983	580.212	
C_{44}	126.780	132.434		114.380	115.002	
C_{66}[a]	134.785	130.628		135.930	116.507	
			Compliance constants (1/GPa)			
S_{11}	0.002 88	0.002 94	0.001 99	0.002 86	0.003 03	
S_{12}	−0.000 83	−0.000 90		−0.000 10	−0.001 27	
S_{13}	−0.000 66	−0.000 71		−0.000 50	−0.000 50	
S_{33}	0.002 54	0.002 45	0.002 12	0.002 06	0.002 01	
S_{44}	0.007 91	0.007 56		0.008 74	0.008 70	
S_{66}[a]	0.007 44	0.007 67		0.007 35	0.008 58	
			Compressibilities (GPa)			
β_v	0.004 06	0.003 70	0.003 55[b]	0.003 76	0.003 53	0.003 90[b]
β_a	0.001 40	0.001 33	0.001 18[b]	0.001 36	0.001 26	0.001 30[b]
β_c	0.001 22	0.001 04	0.001 15[b]	0.001 06	0.001 01	0.001 26[b]
			Young's modulus (GPa)			
5° to ⟨0001⟩	392.287	406.133	456[a]	479.079	490.725	
⟨1$\bar{2}$12⟩	333.555	339.155	378[a]	318.346	308.160	
⟨$\bar{2}$421⟩	345.265	340.082	488[a]	346.209	327.546	
			Velocities of sound (km/s)			
5° to ⟨0001⟩	0.353	0.359	0.385[a]	0.387	0.392	
⟨1$\bar{2}$12⟩	0.325	0.328	0.347[a]	0.316	0.311	
⟨$\bar{2}$421⟩	0.331	0.329	0.394[a]	0.329	0.320	

[a] C_{66} and S_{66} are not independent. $C_{66}=\frac{1}{2}(C_{11}-C_{12})$ and $S_{66}=2(S_{11}-S_{12})$ for a hexagonal system.
[b] References 21 and 24.
[c] Reference 23.

ment in the Mukaseev study and the corresponding velocity of sound, calculated using $E=\rho v^2$ where ρ is the density. To find the experimental velocities, we have taken $\rho=3.14$ g/cm^3 for α silicon nitride and $\rho=3.192$ for β silicon nitride whereas theoretical velocities were calculated using $\rho=3.150$ for α-Si_3N_4 and $\rho=3.191$ for β-Si_3N_4, as obtained from our theoretical crystal structures.

The compressibilities presented in the Jorgensen[21] study are related to the compliance constants by

$$\beta_v=2s_{11}+s_{33}+2s_{12}+4s_{13}\,, \tag{17}$$

$$\beta_a=s_{11}+s_{12}+s_{13}\,, \tag{18}$$

$$\beta_c=2s_{13}+s_{33}\,. \tag{19}$$

Given the small amount of experimental data available, the agreement with theory is reasonable. For example, for β-Si_3N_4 at 300 K, we calculate $\beta_v=0.003\,76$ GPa, $\beta_a=0.001\,36$, and $\beta_c=0.001\,06$, whereas the experiments give $\beta_v=0.003\,90$ GPa, $\beta_a=0.001\,30$, and $\beta_c=0.001\,26$. Until a more complete experimental characterization of the elasticity tensor is available the theoretical predictions will serve as the only complete characterization of the elastic moduli.

V. THERMODYNAMICS

Thermodynamic functions (C_v, S, U, and F) for the α and β crystals were calculated by evaluating all vibrational modes for a number of momenta in the Brillouin zone and using the quantum partition function for each (the quasiharmonic approximation). To test for convergence of the thermodynamic data, calculations were performed using varying numbers of points along each reciprocal vector in the Brillouin zone (see Figs. 3 and 4). For the β crystal, Fig. 3 shows that C_v, S, F, and U at 200 K have converged

Reuse of AIP Publishing content is subject to the terms: http://scitation.aip.org/termsconditions. Downloaded to IP: 133.6.143.32 On: Mon, 27 Jun 2016 08:35:53

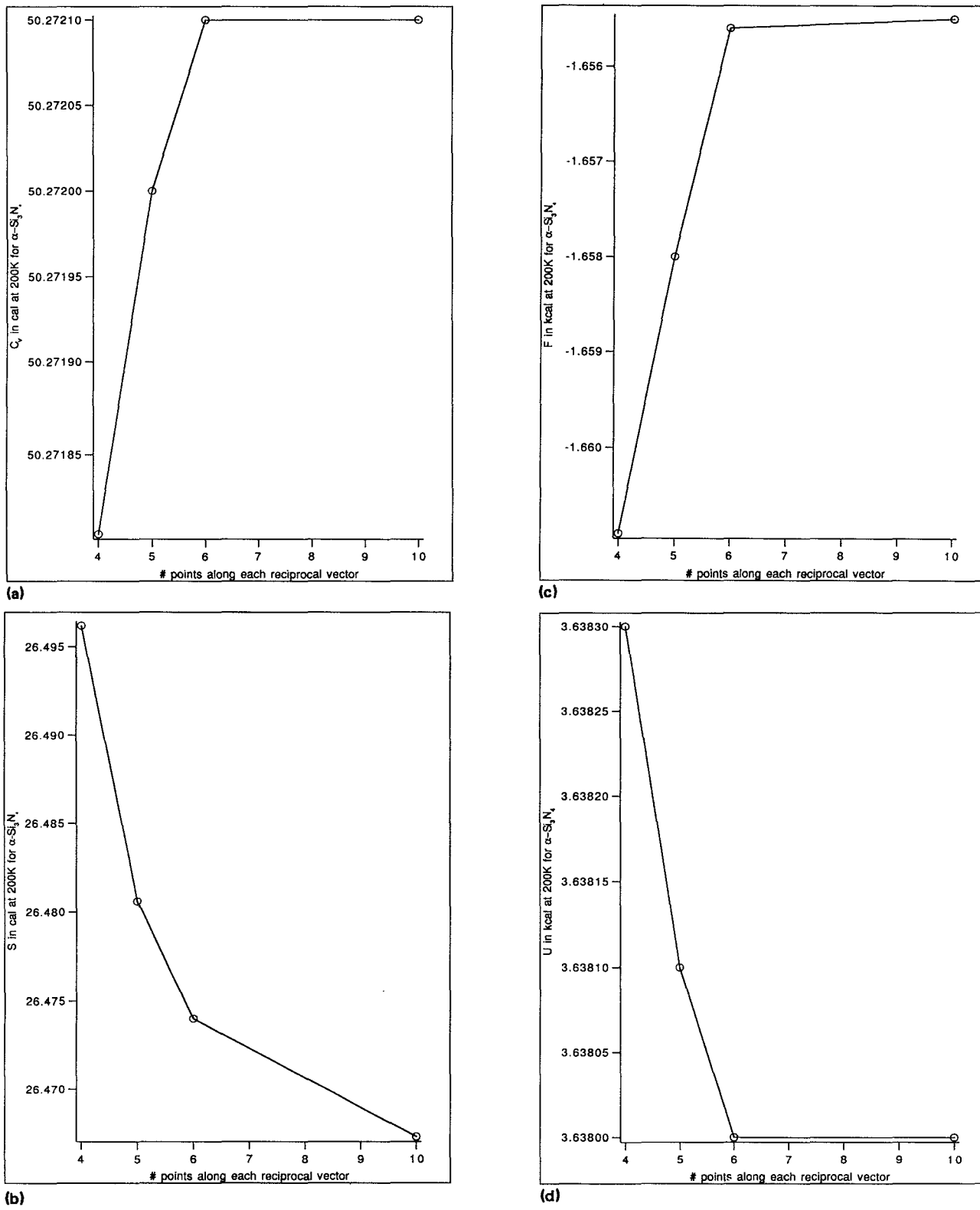

FIG. 3. Convergence of thermodynamic properties of α-Si_3N_4 as a function of the number of points along each reciprocal vector. (a) specific heat, C_v, (b) entropy, S, (c) free energy, F, (d) internal potential energy, U.

when 25 points along each reciprocal vector in the Brillouin zone, a total of $(25)^3 = 15\,625$ points for each temperature. For the α crystal, which has about twice the volume of the β modification, we find (Fig. 4) that 10 points along each vector (1000 points total) are necessary. The final results using 1000 points for α and 15 625 for β are tabulated in Table XII. The experimental data C_p was converted to C_v (the result of our calculations) using C_v

Reuse of AIP Publishing content is subject to the terms: https://publishing.aip.org/authors/rights-and-permissions. Downloaded to IP: 133.6.143.32 On: Mon, 27 Jun 2016 08:35:53

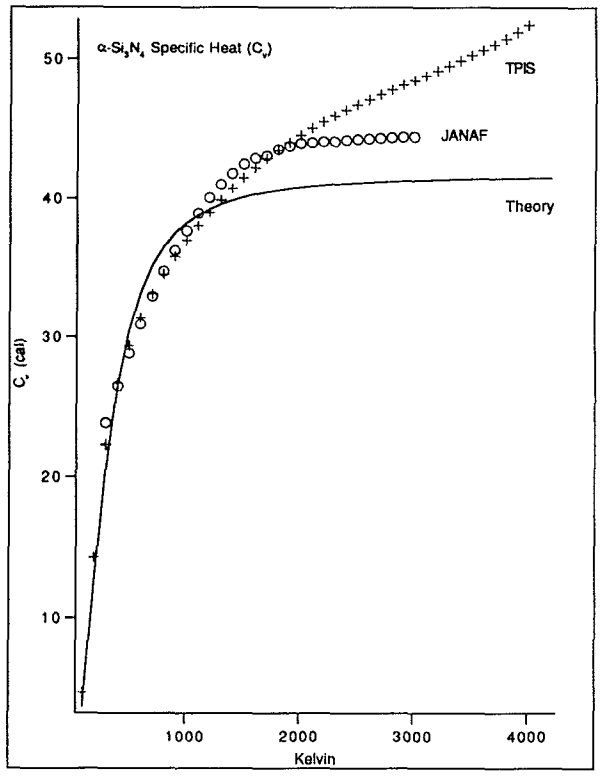

(a)

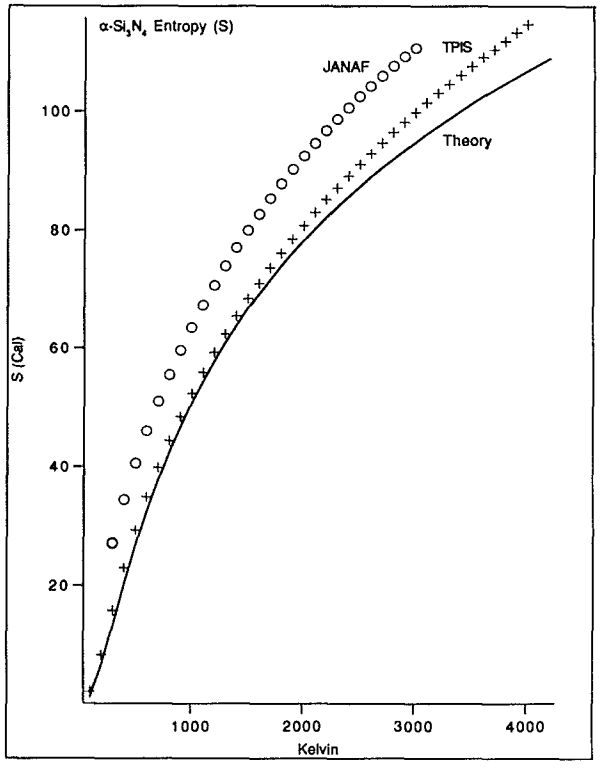

(b)

FIG. 4. Comparison of thermodynamic properties of α-Si_3N_4 from theory and experiment: JANAF Thermochemical Tables (Ref. 26) and Thermodynamic Properties of Individual Substances (Ref. 25). (a) specific heat, C_v, (b) entropy, S.

$=C_p-V\alpha^2T/\beta_v$, where V is the volume, α is the thermal expansion coefficient, and β_v is the volume compressibility. V and β_v were assumed constant and the experimental thermal expansion data[20] was directly interpolated with temperature to obtain α. Data from the JANAF Thermochemical Tables[25] and Thermoproperties of Individual Substances[26] (TPIS) are compared with our calculated results (solid curve) in Fig. 4. Our calculations match the TPIS entropy and C_v data up to 2000 K and and the JANAF C_v data up to about 1500 K. For entropy, the JANAF data differs significantly from TPIS and theory. The deviations at high temperature results because of the use of the quasiharmonic approximation which does not sample the anharmonic regions of the potentials relevant for very high temperatures. (This requires molecular dynamics and will be carried out later.) Summarizing, the theoretical results are well within the experimental error.

Figure 5 shows the temperature dependence for all thermodynamic functions (C_v, S, F, and U) of the α and β phases up to 4000 K. These results indicate essentially identical values for the α and β crystals. This might be expected from the identical bonding and very similar long range crystal structures. The numerical data in Table XII more clearly shows that the β form has a higher entropy and a more negative free energy than the α form over the entire temperature range, although the differences are very small. The higher entropy is due to large channels in the β structure which allow for more vigorous thermal motion than in the α structure. The more negative free energy indicates that the β structure is thermodynamically more stable at all temperatures (by 0.07 kcal/mol at 1000 K). This was unexpected since the α structure is observed as the dominant product in the nitridation of silica and silicon powder below 1700 K.[22] In the presence of molten silicate, a secondary reconstructive transformation from α to β phases takes place.[27] The transition has never been observed in the absence of a liquid phase, which acts as a solvent in which the α-Si_3N_4 can dissolve and recrystallize as β. Likewise, the reverse transition from β to α has never been observed at any temperature. (Previous Madelung energy calculations[28] agree with our thermodynamic results that the β form is more stable at 293 K, well below the observed transition temperature.) These details can be reconciled only if the α phase is kinetically but not thermodynamically favored (as predicted). At the transition temperature, sufficient energy is available to surmount the barrier to the thermodynamically favored β form. The β to α transition does not occur because at the low temperature at which the α and β forms become equally stable thermodynamically (they differ by 0.008 kcal/mol at 300 K) there is not enough energy available to drive the reconstructive transformation, which necessitates full breakdown of the crystal lattice. The reason why temperatures of 1560–1700 K are required for the α to β transition is that solvents suitable for α-Si_3N_4 do not melt until 1500–1700 K.

Reuse of AIP Publishing content is subject to the terms: https://publishing.aip.org/authors/rights-and-permissions. Downloaded to IP: 133.6.143.32 On: Mon, 27 Jun 2016 08:35:53

TABLE XII. Thermodynamic properties of Si_3N_4 (based on 15 625 points in the Brillouin zone for β and 1000 points for α). All functions were calculated per Si_3N_4 formula unit to facilitate comparisons between the α and β modifications. Units are K for temperature; (cal/mol)/K for S and C_v; kcal/mol for F and U.

	Alpha				Beta			
Temp	S	F	C_v	U	S	F	C_v	U
100	1.380 17	−0.035 55	3.654 13	0.102 475	1.416 25	−0.036 7	3.723 8	0.104 95
200	6.616 83	−0.413 875	12.568	0.909 5	6.710 9	−0.421 8	12.640 7	0.920 35
300	13.275 9	−1.404 1	20.499 9	2.578 68	13.384 8	−1.422 5	20.495 8	2.592 9
400	20.026 9	−3.071 3	26.371 4	4.939 45	20.127 5	−3.100 25	26.323 7	4.950 75
500	26.375 2	−5.395 67	30.419 8	7.791 95	26.463 7	−5.434 1	30.360 5	7.797 7
600	32.181 4	−8.328 12	33.183 3	10.980 7	32.259 1	−8.374 85	33.126	10.980 6
700	37.449 4	−11.814	35.101 2	14.400 6	37.518 7	−11.868	35.05	14.395
800	42.230 5	−15.801 8	36.465 6	17.982 6	42.293 4	−15.862 4	36.421 3	17.972 3
900	46.586	−20.245 9	37.462	21.681 5	46.644 1	−20.312 6	37.423 8	21.667 1
1000	50.573 4	−25.106 7	38.207 4	25.466 7	50.627 7	−25.179	38.174 6	25.448 8
1100	54.242 9	−30.35	38.777 5	29.317 2	54.294 2	−30.427 6	38.749 1	29.296 2
1200	57.636 8	−35.946 1	39.222 1	33.218	57.685 9	−36.028 6	39.197 5	33.194 4
1300	60.790 7	−41.869 3	39.575	37.158 5	60.837 9	−41.956 7	39.553 4	37.132 6
1400	63.734 3	−48.097 3	39.859 3	41.130 7	63.78	−48.189 3	39.840 2	41.102 8
1500	66.492 5	−54.61	40.091 5	45.128 7	66.537	−54.706 6	40.074 6	45.098 8
1600	69.086 2	−61.390 3	40.283 5	49.147 7	69.129 7	−61.491 2	40.268 5	49.116 3
1700	71.533 4	−68.422 4	40.443 9	53.184 3	71.576	−68.527 6	40.430 5	53.151 5
1800	73.849	−75.692 5	40.579 3	57.235 7	73.890 9	−75.802	40.567 2	57.201 5
1900	76.046 2	−83.188 2	40.694 5	61.299 5	76.087 5	−83.301 9	40.683 6	61.264 2
2000	78.136 1	−90.898 2	40.793 4	65.374	78.176 9	−91.015 9	40.783 5	65.337 7
2100	80.128 6	−98.812 2	40.878 9	69.457 8	80.168 8	−98.933 9	40.869 8	69.420 5
2200	82.032	−106.921	40.953 3	73.549 4	82.071 8	−107.047	40.944 9	73.511 3
2300	83.853 9	−115.216	41.018 4	77.648 1	83.893 4	−115.346	41.010 7	77.609 2
2400	85.600 9	−123.689	41.075 7	81.752 9	85.640 1	−123.823	41.068 6	81.713 2
2500	87.278 7	−132.339	41.126 3	85.863	87.317 6	−132.471	41.119 8	85.822 7
2600	88.892 6	−141.143	41.171 4	89.978	88.931 3	−141.284	41.165 3	89.937
2700	90.447 2	−150.11	41.211 6	94.097 1	90.485 7	−150.256	41.206	94.055 6
2800	91.946 7	−159.23	41.247 6	98.220 1	91.984 8	−159.38	41.242 4	98.178
2900	93.394 6	−168.498	41.28	102.347	93.432 7	−168.651	41.275 1	102.304
3000	94.794 6	−177.908	41.309 3	106.476	94.832 5	−178.065	41.304 7	106.433
3100	96.149 6	−187.455	41.335 9	110.608	96.187 3	−187.616	41.331 6	110.565
3200	97.462 3	−197.136	41.359 9	114.743	97.499 9	−197.301	41.355 9	114.699
3300	98.735 4	−206.946	41.381 9	118.88	98.772 9	−207.114	41.378 1	118.836
3400	99.971 1	−216.882	41.402	123.019	100.008	−217.054	41.398 4	122.975
3500	101.171	−226.94	41.420 4	127.161	101.209	−227.115	41.417	127.115
3600	102.339	−237.115	41.437 3	131.303	102.376	−237.294	41.434 1	131.258
3700	103.474	−247.406	41.452 8	135.448	103.511	−247.589	41.449 8	135.402
3800	104.58	−257.809	41.467 2	139.594	104.617	−257.996	41.464 4	139.548
3900	105.657	−268.321	41.480 5	143.741	105.694	−268.512	41.477 8	143.695
4000	106.707	−278.94	41.492 8	147.89	106.744	−279.134	41.490 2	147.844
4100	107.732	−289.662	41.504 2	152.04	107.769	−289.86	41.501 7	151.993
4200	108.732	−300.485	41.514 8	156.191	108.769	−300.687	41.512 5	156.144

VI. PHONONS

Given the $P3_1c$ space group for α-Si_3N_4, group theoretical analysis yields

$$\Gamma_{\text{acoustic}}=A_1+E, \tag{20}$$

$$\Gamma_{\text{optic}}=13A_1+14A_2+27E, \tag{21}$$

where the A_1 and E optical modes are active in the IR and Raman, and the A_2 modes are inactive. Because the α crystal structure lacks inversion symmetry, the IR and Raman modes are not mutually exclusive, and a total of 40 modes is predicted for both the IR and Raman. Similarly, the $P6_3/m$ space group for β-Si_3N_4 gives

$$\Gamma_{\text{acoustic}}=A_u+E_{1u}, \tag{22}$$

$$\Gamma_{\text{optic}}=4A_g+3B_g+2E_{1g}+5E_{2g}+2A_u+4B_u+4E_{1u}+2E_{2u}, \tag{23}$$

Reuse of AIP Publishing content is subject to the terms: https://publishing.aip.org/authors/rights-and-permissions. Downloaded to IP: 133.6.143.32 On: Mon, 27 Jun 2016 08:35:53

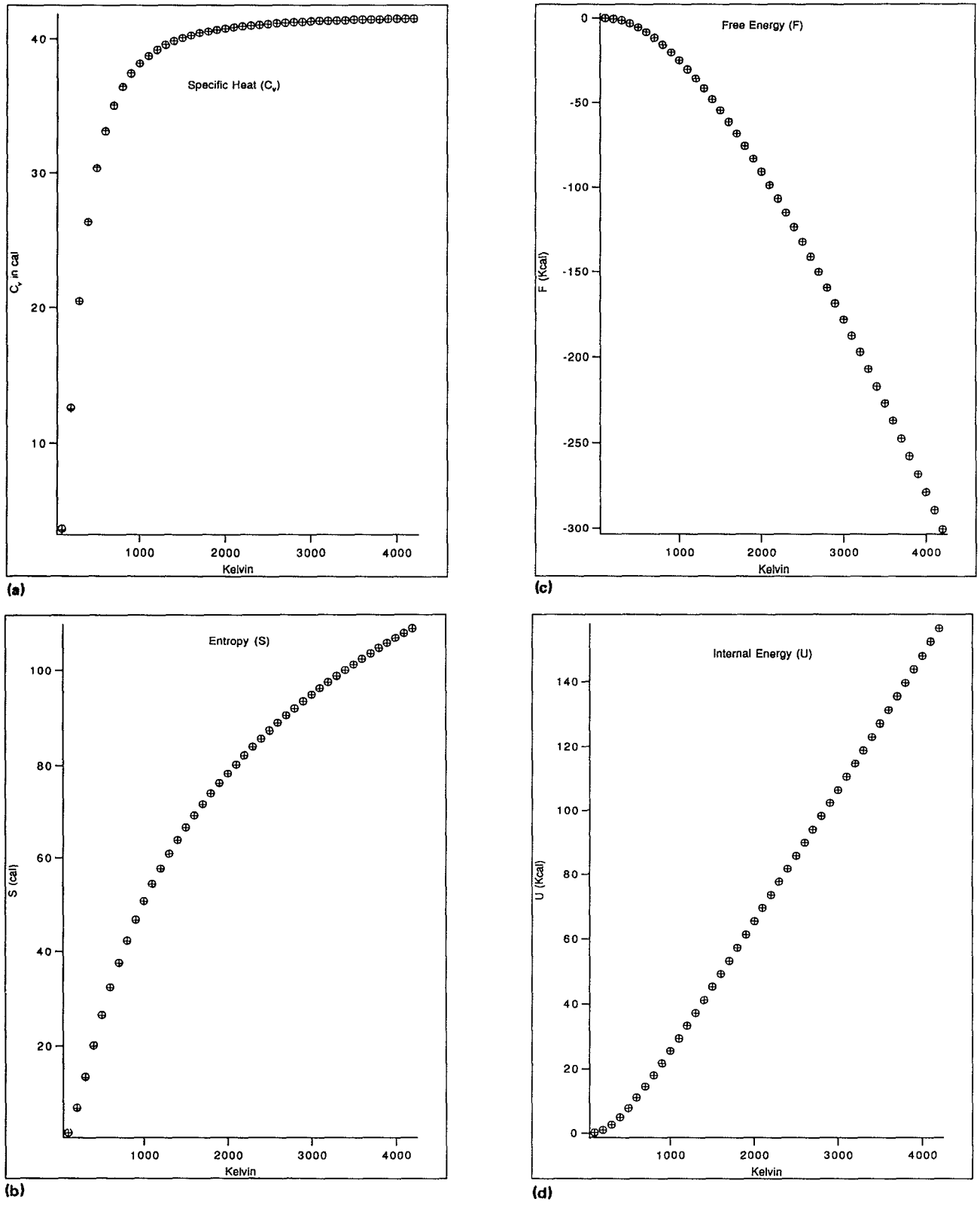

FIG. 5. Comparison of thermodynamic properties for α and β-Si_3N_4. (a) specific heat, C_v, (b) entropy, S, (c) free energy, F, (d) internal potential energy, U.

where the 11 A_g, E_{1g}, and E_{2g} modes are Raman active and the 6 A_u and E_{1u} modes are IR active. Our calculated IR and Raman spectra are shown in Table XIII. Although Wada[29] has carried out measurements of these spectra at the Γ point, no mode assignments have been made to his data, so comparisons with our theoretical predictions are difficult. The 42 phonon bands of β-Si_3N_4 and 84 phonon bands of α-Si_3N_4 are shown from the zone center of $[\pi/$

Reuse of AIP Publishing content is subject to the terms: https://publishing.aip.org/authors/rights-and-permissions. Downloaded to IP: 133.6.143.32 On: Mon, 27 Jan 2020 08:33:33

TABLE XIII. Predicted IR and Raman phonon energies (cm^{-1}) at the Γ point for Si_3N_4 crystal.

Alpha IR and Raman		Beta IR		Beta Raman	
Mode	Symmetry	Mode	Symmetry	Mode	Symmetry
202	E	481	E_{1u}	190	E_g
252	A_1	548	A_u	215	E_g
261	A_1	580	E_{1u}	236	A_g
282	A_1	1012	E_{1u}	289	A_g
294	E	1062	A_u	518	E_g
315	E	1064	E_{1u}	539	A_g
331	E			547	A_g
372	E			592	E_g
394	E			975	E_g
400	A_1			1017	E_g
443	E			1067	E_g
500	E				
512	A_1				
538	A_1				
541	E				
547	A_1				
553	E				
575	E				
592	E				
604	A_1				
647	A_1				
687	E				
701	A_1				
875	E				
899	E				
965	E				
965	A_1				
982	E				
998	E				
1003	A_1				
1004	E				
1011	E				
1030	E				
1052	E				
1058	E				
1068	A_1				
1079	E				
1084	E				
1090	A_1				

$2a,0,0]$ and $[0,0,\pi/2a]$ are shown in Figs. 6 and 7 for α and β, respectively. The composite phonon bands for these hexagonal systems are shown in Fig. 8. These results should be useful as a guide to future experimental studies.

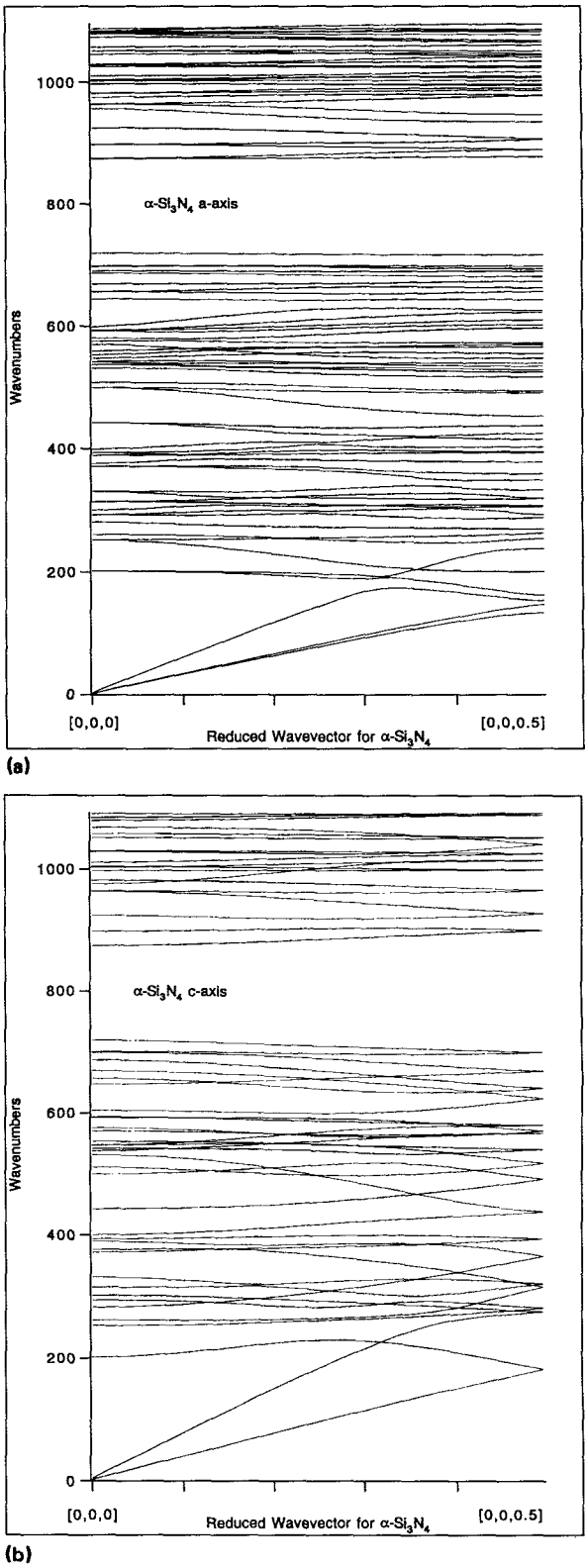

FIG. 6. Calculated phonon dispersion curves for α-Si_3N_4. Tne abscissa is in reduced units, ka/π or kc/π. (a) along $[k_x,0,0]$, (b) along $[0,0,k_z]$.

VII. SUMMARY

Force fields for the α and β forms of silicon nitride were calculated using the Hessian biased approach and *ab initio* calculations on the $N(SiH_3)_3$ and $Si(NH_2)_4$ clusters. Optimized crystal structures were obtained using conjugate gradient techniques; elastic constants, thermodynamic properties, and phonon bands were calculated using analytic second derivatives; and theoretical lattice expansion curves were obtained by performing molecular dynamics runs on extended structures at various temperatures. We find good agreement with experimental results for crystal structures, lattice expansion parameters, and the thermo-

Reuse of AIP Publishing content is subject to the terms: https://publishing.aip.org/authors/rights-and-permissions. Downloaded to IP: 133.6.143.32 On: Mon, 27 Jun 2016 08:35:53

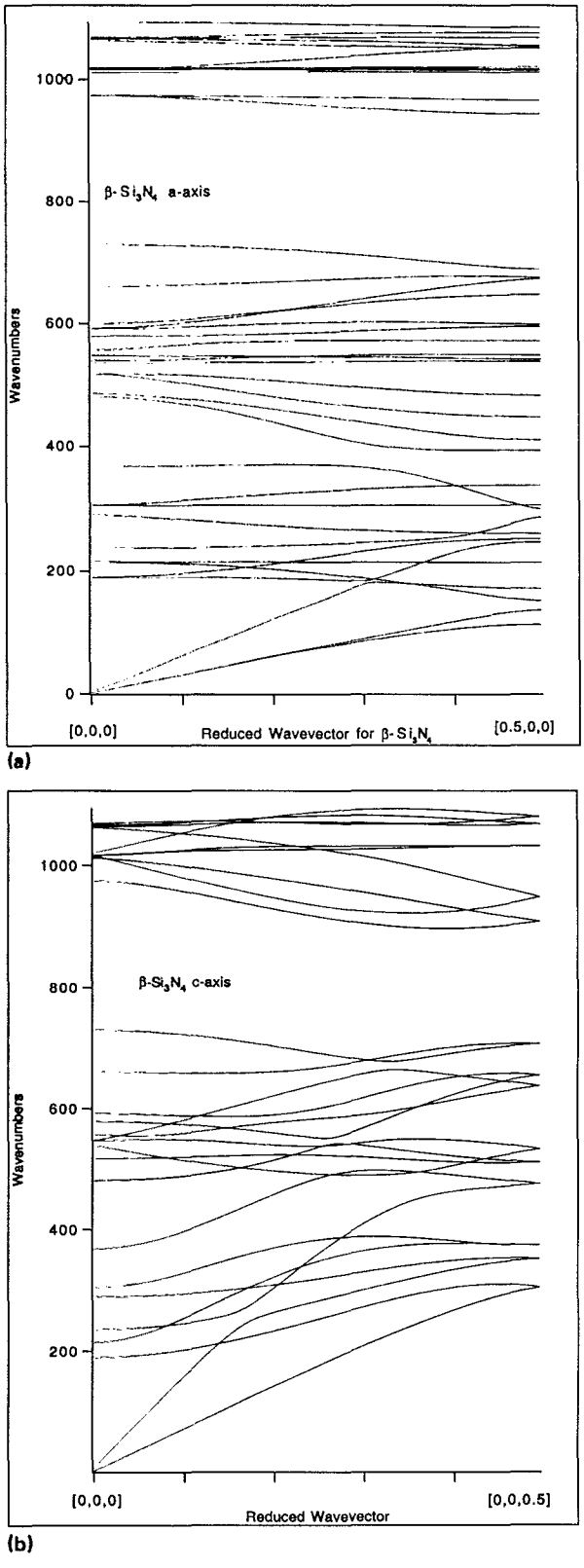

FIG. 7. Calculated phonon dispersion curves for β-Si_3N_4. The abscissa is in reduced units, ka/π or kc/π. (a) along $[k_x,0,0]$, (b) along $[0,0,k_z]$.

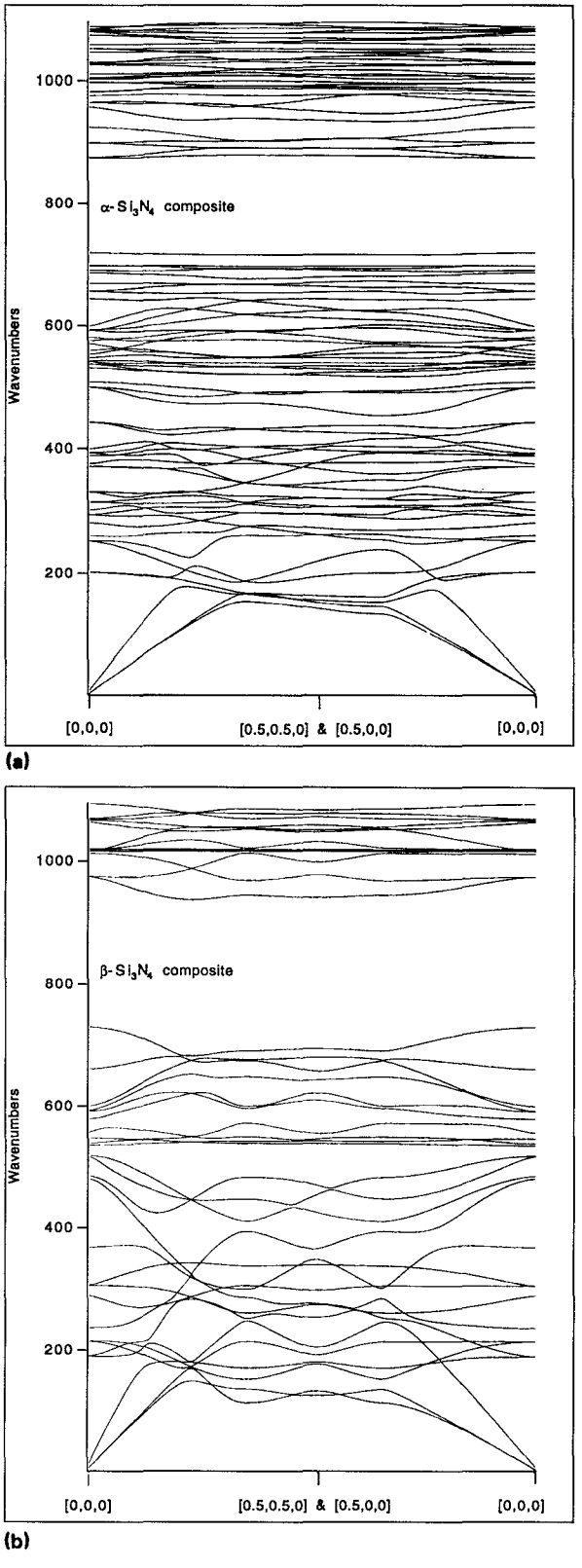

FIG. 8. Composite phonon dispersion curves for $[000]\rightarrow[\frac{11}{22}0]$, $[\frac{1}{2}00]\rightarrow[000]$ for (a) α-Si_3N_4, (b) β-Si_3N_4.

dynamics functions C_v and S. The measurements of elastic constants are insufficient for rigorous comparison with our theory; however, the theory agrees well with current data.

We find that β-Si_3N_4 is thermodynamically more stable than α-Si_3N_4 over the entire temperature range tested (0–4200 K). This indicates that the observed formation of α-Si_3N_4 at temperatures below 1500 K occurs for kinetic reasons. This accounts for the currently unexplained lack

Reuse of AIP Publishing content is subject to the terms: https://publishing.aip.org/authors/rights-and-permissions. Downloaded to IP: 133.6.143.32 On: Mon, 27 Jun 2016 08:35:53

of a β to α transition.

ACKNOWLEDGMENTS

The research was initiated with a grant (ASOFR-88-0051) from the Air Force Office of Scientific Research. It was completed with support from the National Science Foundation (CHE-91 100284) and from Allied-Signal Corp. The computer facilities of the Materials and Molecular Simulation Center (MSC) of the Beckman Institute were supported by Allied-Signal, Asahi Chemical, Asahi Glass, and Chevron plus grants from DOE-AICD and DARPA/ONR. All force field and molecular dynamics calculations used PolyGraf (from Molecular Simulation Inc., Waltham, Massachusetts) plus software developed at the MSC for optimizing force fields (Ref. 13) and for calculating elastic constants and phonon states (Ref. 3). All quantum chemical calculations used GAUSSIAN 90 (Ref. 10). The calculations were carried out on FPS522, Alliant FX80/8, and Silicon Graphics 380 computers.

[1] R. N. Katz, Science **208**, 841 (1980).
[2] A. K. Rappe and W. A. Goddard III, J. Phys. Chem. **95**, 3358 (1991).
[3] N. Karasawa and W. A. Goddard III (to be published); see N. Karasawa, Ph.D. thesis, Applied Physics, Caltech, November 1991.
[4] N. Karasawa, S. Dasgupta, and W. A. Goddard III, J. Phys. Chem. **95**, 2260 (1991).
[5] S. L. Mayo, B. D. Olafson, and W. A. Goddard III, J. Phys. Chem. **92**, 7488 (1990).
[6] N. Karasawa and W. A. Goddard III (to be published).
[7] S. Dasgupta and W. A. Goddard III, J. Chem. Phys. **90**, 7207 (1989).
[8] T. D. Goldfarb and B. N. Khare, J. Chem. Phys. **46**, 3379 (1967).
[9] F. A. Miller, J. Perkins, G. A. Gibbon, and B. A. Swisshelm, J. Raman Spectrosc. **2**, 93 (1974).
[10] GAUSSIAN 90, Revision F, M. J. Frisch, M. Head-Gordon, G. W. Trucks, J. B. Foresman, H. B. Schlegal, K. Raghavachari, M. Robb, J. S. Binkley, C. Gonzalez, D. J. Defrees, D. J. Fox, R. A. Whiteside, R. Seeger, C. F. Melius, J. Baker, R. L. Martin, L. R. Kahn, J. J. P. Stewart, S. Topial, and J. A. Pople (Gaussian, Inc., Pittsburgh, 1990).
[11] K. Hedberg, J. Am. Chem. Soc. **77**, 6491 (1955).
[12] B. Beagley and K. Conrad, Trans. Faraday Soc. **66**, 2740 (1970).
[13] T. Yamasaki, S. Dasgupta, and W. A. Goddard III (to be published).
[14] H. F. Shurvell, A. Dunham, S. J. Cyvin, and J. Brunvoll, Can. J. Chem. **57**, 1779 (1979).
[15] D. L. Smith, A. S. Alimonda, C. C. Chen, S. E. Ready, and B. Wacker, J. Electrochem. Soc. **137**, 614 (1990).
[16] I. W. Levin and W. T. King, J. Chem. Phys. **37**, 1375 (1962).
[17] J. L. Duncan and I. M. Mills, Spectrochim. Acta. **20**, 523 (1964).
[18] S. Wild, P. Grieveson, and K. H. Jack, Symp. Spectrosc. Ceram. **5**, 385 (1972).
[19] K. Kato, Z. Inoue, K. Kijima, I. Kawada, H. Tanaka, and T. Yamane, J. Am. Ceram. Soc. **58**, 90 (1975).
[20] *Thermal Expansion: Nonmetallic Solids*, TPRC Data Series, Vol. 13, edited by Y. S. Toulokian, R. K. Kirby, R. E. Taylor, and T. Y. K. Lee (Plenum Publishing Corporation, New York, 1972), p. 1140.
[21] L. Cartz and J. D. Jorgensen, J. Appl. Phys. **52**, 236 (1981).
[22] *Structural Ceramics*, edited by J. B. Wachman, Jr. (Academic, New York, 1989), Chap. 4.
[23] A. A. Mukaseev, V. N. Gribkov, B. V. Shchetanov, A. S. Isaikin, and V. A. Silaev, Poroshk. Metall. **12**, 97 (1972).
[24] S. R. Srinivasa, Ph.D. thesis, Marquette University, 1977 (unpublished), cited by Ref. 19.
[25] *Thermodynamic Properties of Individual Substances*, 4th ed., edited by L. V. Gurvich, I. V. Veyts, and C. B. Alcock (Hemisphere Publishing Company, New York, 1989).
[26] *JANAF Thermochemical Tables*, 3rd ed., edited by M. W. Chase, Jr., C. A. Davies, J. R. Downey, Jr., D. J Frurip, R. A. McDonald, and A. N. Syverad (American Chemical Society, New York, 1985).
[27] J. Y. Park, C. H. Kim, J. Mater. Sci. **23**, 1988, 3049.
[28] R. Grun, Acta Crystallogr. B **35**, 800 (1979).
[29] N. Wada, S. A. Solin, J. Wong, and S. Prochazka, J. Non-Cryst. Solids **43**, 7 (1981).

Reuse of AIP Publishing content is subject to the terms: http://scitation.aip.org/termsconditions. Downloaded to IP: 133.6.143.32 On: Mon, 27 Jun 2016 08:35:53